

# Primordial black holes from an aborted phase transition

Wen-Yuan Ai,<sup>1,\*</sup> Lucien Heurtier,<sup>1,†</sup> and Tae Hyun Jung<sup>2,‡</sup>

<sup>1</sup>*Theoretical Particle Physics and Cosmology,*

*King's College London, Strand, London WC2R 2LS, UK*

<sup>2</sup>*Particle Theory and Cosmology Group, Center for Theoretical Physics of the Universe,  
Institute for Basic Science (IBS), Daejeon, 34126, Korea*

We propose a new mechanism of primordial black hole formation via an aborted phase transition during the early matter-dominated stage of reheating after inflation. In reheating, induced by the decay of a pressureless fluid dominating the Universe at the end of inflation, dubbed as reheaton, the temperature of the radiation bath typically increases, reaching a maximum temperature  $T_{\max}$ , and then decreases. We consider a first-order phase transition induced by the increase of the temperature that is aborted as  $T_{\max}$  is higher than the critical temperature but not sufficiently high for the bubble nucleation rate to overcome the expansion of the Universe. Although bubbles never fully occupy the space, some may be nucleated and expand until the temperature once again decreases to the critical temperature. We argue that these bubbles shrink and disappear as the temperature drops further, leaving behind macroscopic spherical regions with positive density perturbations. These perturbed regions accrete the surrounding matter (reheatons) and eventually collapse into primordial black holes whose mass continues to grow until the onset of radiation domination. We estimate the abundance of these primordial black holes in terms of the bubble nucleation rate at  $T_{\max}$ , and demonstrate that the abundance can be significantly large from a phenomenological perspective.

**Introduction**—Primordial black holes (PBHs) are black holes that form in the early Universe in a non-stellar way (see Ref. [1] for a recent review). Their possible existence throughout cosmic history has rich phenomenological implications [1–3] and a broad mass range of PBHs are compelling candidates for the dark-matter component of the Universe [4–6] that might be on the verge of being probed using solar ephemerides precision measurements [7, 8]. Moreover, PBHs could also explain a variety of conundrums, including the recently observed microlensing signal candidates, the correlations in the cosmic infrared and X-ray backgrounds, and the origin of the supermassive black holes in galactic nuclei at high redshift [9]. Moreover, it is possible that the LIGO/Virgo black hole mergers [10, 11] has a primordial origin [12].

So far, most of the PBH formation mechanisms involved the gravitational collapse of large curvature perturbations generated during inflation. To generate such large curvature perturbations, the inflation model is required to have peculiar features, e.g., an inflection point or a plateau in a small field range of the potential [5, 13–22], a potential hill [23–26], multiple phases of inflation or hybrid inflation [27–38], a non-canonical kinetic term [39, 40], multifield inflation [41, 42], light spectator fields [43–46], and other possibilities (e.g. [47–49]). In addition, PBH formation has been considered in connection with preheating after inflation [50–53] although their formation in this context was recently questioned [54].

Long after the idea was suggested in Refs. [55, 56], recent works reconsidered that PBHs may also be formed from a first-order phase transition (FOPT) [57–62]. This

idea was then further investigated in Refs. [63–77]. This possibility is particularly exciting, as FOPTs are naturally present in many particle physics models and have far-reaching phenomenological consequences, such as the emission of a stochastic gravitational wave background.

In this *Letter*, we propose a new PBH formation mechanism in which an FOPT occurs while the Universe's temperature increases during reheating after inflation. This FOPT is thus a heating phase transition [78–80] rather than a cooling phase transition that occurs as the temperature decreases in the early Universe. The special ingredient of our scenario is an abortion of the FOPT assuming that the maximal temperature reached in reheating is higher than the critical temperature but lower than the temperature that guarantees the phase transition to complete. In the following, we introduce the specifics of the aborted phase transition, explain how PBH can form in this setup, and relate the PBH mass and abundance to the dynamics of the perturbative reheating and the phase transition sector considered.

**Reheating sector**—Before going into the details, let us be clear in our setup. When inflation ends, we consider the Universe to be filled with a pressureless fluid slowly decaying into particles that quickly get thermalized, producing a relativistic plasma. We refer to this decaying matter component as the *reheaton*,  $\chi$ . As  $\chi$  decays, the radiation sector's temperature first increases, reaching the maximal temperature  $T_{\max}$ , and decreases as the Universe expands. The temperature evolution in terms of the scale factor  $a$  can be described by [81]

$$T(a) = c_1 T_{\max} \left[ \left( c_2 \frac{a}{a_{\max}} \right)^{-\frac{3}{2}} - \left( c_2 \frac{a}{a_{\max}} \right)^{-4} \right]^{\frac{1}{4}}, \quad (1)$$

where  $a_{\max}$  is the scale factor at  $T = T_{\max}$ ,  $c_1 = 2^{6/5} (27^{1/5} 5)^{-1/4} \approx 1.30$  and  $c_2 = 2^{6/5} 3^{-2/5} \approx 1.48$ .

\* wenyuan.ai@kcl.ac.uk

† lucien.heurtier@kcl.ac.uk

‡ thjung0720@gmail.com

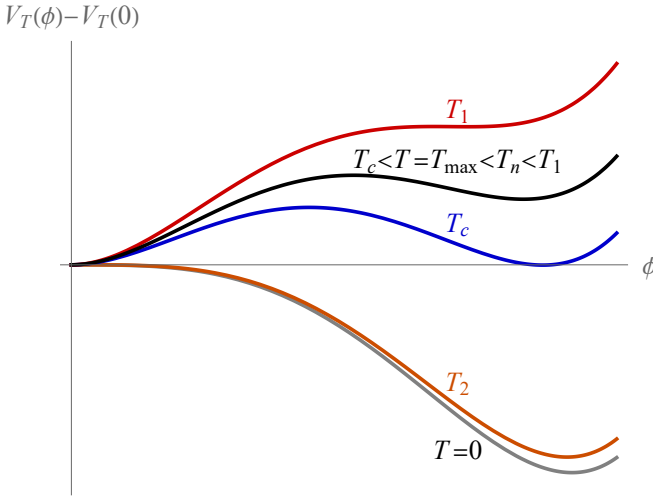


FIG. 1. An example of the temperature dependence of scalar potential.

Denoting by  $\Gamma_x$  the decay width of the reheaton, matter domination lasts until the plasma temperature reaches the reheating temperature  $T_{\text{RH}} \sim \sqrt{\Gamma_x M_{\text{Pl}}}$ , with  $M_{\text{Pl}} = 2.4 \times 10^{18}$  GeV being the reduced Planck mass, below which radiation domination starts. In general, there is no direct relation between  $T_{\text{RH}}$  and  $T_{\text{max}}$ , as the value of the latter depends on the time at which the reheating starts, so it is natural to assume that there is a large hierarchy between them.

**Aborted phase transition**—Now, let us consider a real scalar field  $\phi$  which breaks a symmetry<sup>1</sup>, spontaneously, by getting a nonzero vacuum expectation value. Assuming that the scalar sector undergoes an FOPT along the temperature change, one can define three characteristic temperatures that play an important role: the critical temperature,  $T_c$  at which two local minima are degenerate, the spinodal (binodal) temperature  $T_1$  ( $T_2$ ) above (below) which the potential barrier disappears (see Fig. 1 for the schematic description of thermal effective potential  $V_T(\phi)$  at each temperature). During inflation, the temperature is zero, and  $\phi$  is stabilized in the symmetry-breaking vacuum assuming that the inflation scale is not too large compared to the curvature scale of the potential.

While the thermal bath is heated, the scalar potential  $V(\phi)$  receives thermal corrections and there can be two types of phase transitions in general. During the change of  $T = 0 \rightarrow T_{\text{max}} > T_c$ , the symmetry-restoring vacuum becomes more stable compared to the symmetry-breaking vacuum, and the phase transition occurs. This

phase transition is called *symmetry-restoring*, or heating phase transition (see, e.g. Ref. [78–80], for related discussions in various contexts). In previous studies, it is assumed that the heating phase transition is completed and that the Universe settles down in the symmetry-restoring phase. Then, as the temperature drops back, the symmetry-breaking vacuum becomes more stable again, and the symmetry-breaking (or cooling) phase transition starts at the bubble nucleation temperature.

On the contrary, in this *Letter*, we assume that  $T_{\text{max}}$  is greater than the critical temperature  $T_c$ , but not large enough to make the bubble nucleation rate catch up with the spacetime expansion. Thus, the phase transition is *aborted* at  $T_{\text{max}}$  by the temperature's turning around. Bubbles can still be formed, but since they never collide with each other, they just expand during  $T > T_c$  and shrink back when  $T < T_c$ . We argue that these bubbles eventually lead to PBH formation and that the abundance of such PBHs can be significant.

**Fate of bubbles in the aborted phase transition**—Initially, the bubble grows since the free energy density difference,  $\Delta V_T \equiv V_T(\phi_b) - V_T(\phi_s)$ , is positive, where  $\phi_b$  and  $\phi_s$  denote the symmetry-breaking and restoring extrema of the thermal effective potential, respectively. Once the wall starts expanding, the perturbed plasma would backreact to the wall, creating a backreaction force  $\mathcal{P}_{\text{back}}(v_w)$ , which has a dependence on the wall velocity. In general, a terminal velocity exists and should be reached after a short acceleration period, determined by  $\Delta V_T = \mathcal{P}_{\text{back}}(v_w)$  [79, 80].

As the temperature changes,  $\Delta V_T$  also changes, so the wall velocity adiabatically follows the terminal velocity at each temperature; it reaches a maximal value at  $T_{\text{max}}$  and decreases as  $T$  decreases. At  $T = T_c$ , since the terminal velocity becomes  $v_w = 0$  by definition, this is the moment when the bubble stops expanding and has the largest comoving radius, which we denote as  $r_{c,2}$ . The subscript  $c,2$  will be used to indicate quantities estimated at the critical temperature reached for the second time throughout this *Letter*. The critical temperature was reached for the first time during the temperature-increasing process,  $T = 0 \rightarrow T_{\text{max}}$ , for which we use the labeling of  $c,1$ .

We can estimate  $r_{c,2}$  as  $r_{c,2} = \int_{t_{\text{nuc}}}^{t_{c,2}} dt' v_w(t')/a(t') \sim \bar{v}(\eta_{c,2} - \eta_{\text{nuc}})$  where  $\eta$  is the conformal time defined via  $dt = ad\eta$ ,  $\bar{v}$  denotes the averaged wall velocity in bubble expansion, and the subscript  $\text{nuc}$  indicates quantities estimated at the time when this bubble is nucleated. In a matter-dominated universe, we have  $H(a) \propto a^{-3/2}$  and thus

$$r_{c,2} \sim \bar{v}(\eta_{c,2} - \eta_{\text{nuc}}) = \frac{2\bar{v}}{a_{c,2} H_{c,2}} \left[ 1 - \left( \frac{a_{\text{nuc}}}{a_{c,2}} \right)^{\frac{1}{2}} \right]. \quad (2)$$

This shows that the comoving radius at  $t_{c,2}$  is of the order of the comoving Hubble radius  $r_H = 1/(aH)$ .

Afterwards, at  $T < T_c$ , the net pressure  $\Delta V_T$  becomes negative, and the bubble starts shrinking. The bubble wall velocity stays following its terminal (negative) velocity, which induces fluid motion of the plasma in this

<sup>1</sup> The symmetry in our scenario actually does not play any role, and it is conceivable that a phase transition does not involve any symmetry being restored or broken. However, we will maintain this terminology of symmetry restoration/breaking throughout for the sake of intuitive discussion.

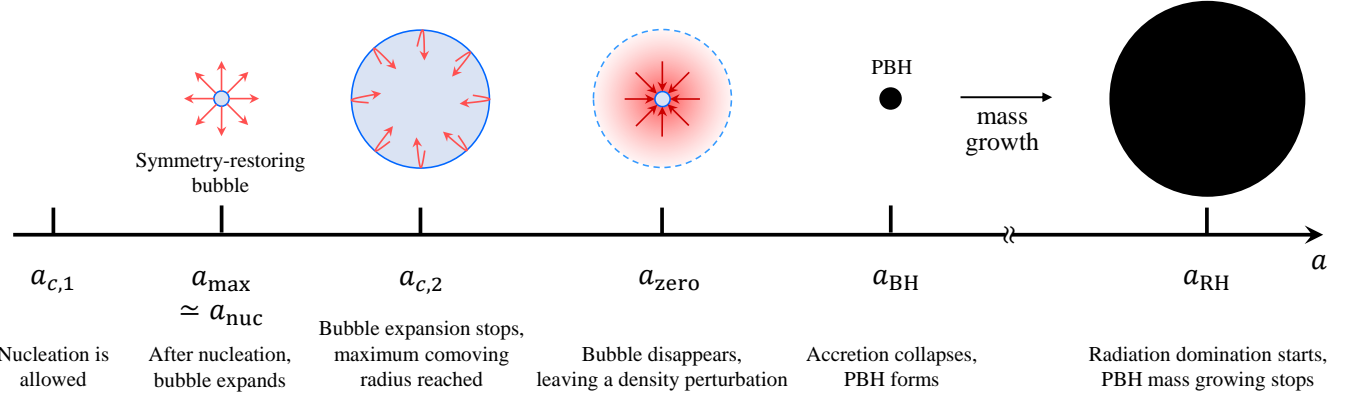


FIG. 2. A schematic chronology of our PBH formation scenario. A symmetry-restoring bubble nucleates at around  $a_{\max}$  and expands with the bubble wall indicated by the blue line. At  $a_{c,2}$ , the bubble wall stops expanding, turns around, and shrinks until it completely disappears at  $a_{\text{zero}}$ . This leaves a spherical overdense region of macroscopic size (dashed blue line). This region accretes surrounding matter (reheaton), and the accretion collapses into a PBH via the post-collapse accretion mechanism at  $a_{\text{BH}}$ . The PBH mass grows until the radiation domination starts at  $a_{\text{RH}}$ .

region. This shrinking occurs slightly below  $T_c$ , while the vacuum energy difference is comparable to the pressure of the radiation plasma. Therefore, the bubble wall does not run away, as shown in more detail in the supplementary material, Section S2. In the absence of any runaway during both its expansion and contraction phases, the energy budget of the bubble wall's kinetic motion is negligible. To understand what happens in this region, we can thus focus on the balance between vacuum and thermal energy, where the latter should be understood to include the fluid's bulk motion. During bubble expansion, i.e. when  $T > T_c$ , the thermal energy is first transferred into vacuum energy which redshifts slower than the radiation plasma with cosmic expansion. Later on, the bubble's contraction at  $T < T_c$  converts vacuum energy back to thermal energy. Therefore, the energy density of the region perturbed by the wall's motion is greater than the unperturbed region far away from the nucleation site.

Because the Universe is still matter-dominated as we assume  $T_{\max} \gtrsim T_c \gg T_{\text{RH}}$ , the presence of such an overdensity easily leads to PBH formation via the post-collapse accretion mechanism [82–84] (see also Refs. [53, 84–96] for PBH formation during matter domination in a variety of different aspects). After the bubble completely disappears, the overdense region, with a macroscopic size as large as the comoving radius  $r_{c,2}$  defined in Eq. (2), creates a gravitational potential and triggers an accretion of reheaton into this region. The accretion of the reheaton (which is pressureless in our setup) finally leads to the whole region collapsing into a black hole with an initial mass of order  $10^{-2} M_H$  [82] where  $M_H = 4\pi M_{\text{Pl}}^2/H$  is the Hubble mass for a given background expansion rate  $H$ . As shown in Ref. [82], after it forms, the black hole quickly increases in mass by absorbing the surrounding matter. Once the PBH mass reaches about one Hubble mass, the rapid accretion is expected to be slowed down, and the mass simply follows the scaling of one

Hubble mass  $M_{\text{BH}} \sim M_H \propto a^{3/2}$ . This mass-growing process ends when radiation domination starts. Eventually, the final PBH mass is simply determined by the value of the Hubble mass at the time of the reheating, which we evaluate by considering that there is a matter-radiation equality at  $T_{\text{RH}}$ , giving

$$M_{\text{PBH}} \sim 3.5 \times 10^{-12} M_{\odot} \alpha \left( \frac{10^5 \text{ GeV}}{T_{\text{RH}}} \right)^2 \left( \frac{100}{g_*(T_{\text{RH}})} \right)^{1/2}, \quad (3)$$

where  $g_*(T_{\text{RH}})$  is the number of effective relativistic degrees of freedom present in the plasma at the reheating time, and  $\alpha \lesssim 1$  is an efficiency factor, which we take to be  $\mathcal{O}(0.1)$  for simplicity. As can be seen from Eq. (3),  $M_{\text{PBH}}$  is insensitive to the phase transition properties and solely determined by the value of  $T_{\text{RH}}$  once they are formed. The distribution of PBHs formed from an aborted phase transition is thus expected to be monochromatic.

Note that the time scale of the PBH formation and mass-growing process is around the Hubble time scale [82, 84] at the time when the density perturbation is generated. Therefore, as long as  $T_{\max} \gtrsim T_c \gg T_{\text{RH}}$ , there is enough time for the PBH to form and grow. The chronology of our PBH formation scenario is schematically summarized in Fig. 2, where one can also check our notations for important events.

**PBH abundance**—The PBH relic abundance can be estimated by counting the expected number of symmetry-restoring bubble nucleations during the aborted phase transition. It is thus sensitive to the bubble nucleation rate per unit volume,  $\Gamma(T) \sim T^4 e^{-S_3/T}$  where  $S_3$  is the minimal energy of the scalar configuration to make a thermal escape from the local minimum, which can be obtained by the three-dimensional Euclidean action of the  $O(3)$  bounce solution [97–99]. Since the phase transition is aborted,  $\Gamma$  is maximized at the moment where

$T = T_{\max}$ , and most of the symmetry-restoring bubbles are nucleated around this time.

To be specific, let us consider a sufficiently large comoving total volume  $\bar{V}$ . The number of nucleated bubbles at time  $t_{\text{nuc}}$ , corresponding to  $a_{\text{nuc}}$ , is given by

$$dN_{\text{PBH}}(a_{\text{nuc}}) = \frac{da_{\text{nuc}}}{a_{\text{nuc}} H(a_{\text{nuc}})} \times \bar{V} a_{\text{nuc}}^3 \Gamma(T(a_{\text{nuc}})). \quad (4)$$

Integrating it from  $t_{c,1}$  to  $t$  and dividing the result by  $\bar{V} a(t)^3$  gives the integrated number density at  $t$

$$n_{\text{PBH}}(t) = \left( \frac{a_{\max}}{a(t)} \right)^3 \int_{a_{c,1}}^{a(t)} \left( \frac{a_{\text{nuc}}}{a_{\max}} \right)^2 \frac{\Gamma(T(a_{\text{nuc}})) da_{\text{nuc}}}{a_{\max} H(a_{\text{nuc}})}. \quad (5)$$

From this, one can obtain the PBH dark matter fraction  $f_{\text{PBH}} = n_{\text{PBH}}(t_{\text{today}}) M_{\text{PBH}} / (\rho_c \Omega_{\text{DM}})$ .

Here, we proceed with a rough estimation using a model-independent approach with the following approximations. First of all, we take the Taylor expansion of  $S_3/T$  around  $T_{\max}$  in the log scale;

$$\frac{S_3}{T} \simeq \frac{S_3}{T} \bigg|_{T=T_{\max}} - \hat{\beta}_{\max} \ln \left( \frac{T}{T_{\max}} \right), \quad (6)$$

where we define the rapidity parameter  $\hat{\beta}_{\max}$  as

$$\hat{\beta}_{\max} \equiv - \frac{d(S_3/T)}{d \ln T} \bigg|_{T=T_{\max}}. \quad (7)$$

Then we can approximate  $\Gamma(T)$  as  $\Gamma(T) \simeq \Gamma(T_{\max})(T/T_{\max})^{\hat{\beta}_{\max}+4}$ . In the Supplementary Material, we evaluate  $S_3/T$  and  $\hat{\beta}_{\max}$  in the case of the so-called Abelian Higgs model and obtain  $\hat{\beta}_{\max}$  around  $10^4$ – $10^6$ . We use this value as a benchmark in what follows. In addition, using Eq. (1) to evaluate  $T(a)$ , we obtain in the limit  $a \approx a_{\max}$

$$T(a) \simeq T_{\max} \exp \left[ - \frac{3}{4} \left( \frac{a}{a_{\max}} - 1 \right)^2 \right]. \quad (8)$$

Although (7) and (8) are only valid around  $T_{\max}$ , we checked numerically that they lead to a good approximation for  $f_{\text{PBH}}$  as long as  $\hat{\beta}_{\max} > 50$  because the largest contribution to  $f_{\text{PBH}}$  comes from  $\Gamma(T_{\max})$ .

Then, Eq. (5) can be approximated as

$$n_{\text{PBH}}(t_{\text{RH}}) \simeq \sqrt{\frac{4\pi}{3\hat{\beta}_{\max}}} \left( \frac{a_{\max}}{a_{\text{RH}}} \right)^3 \frac{\Gamma(T_{\max})}{H_{\max}}, \quad (9)$$

for  $\hat{\beta}_{\max} > 50$ . Assuming that the PBH yield is unchanged after reheating temperature, we obtain  $f_{\text{PBH}}$  as

$$\begin{aligned} f_{\text{PBH}} &= \frac{M_{\text{PBH}} n_{\text{PBH}}/s}{\rho_{\text{DM}}/s} \\ &\sim 1 \alpha \left( \frac{T_{\text{RH}}}{10^5 \text{ GeV}} \right) \left( \frac{\left( \frac{\Gamma(T_{\max})}{H_{\max}^4} \right)}{10^{-16}} \right) \left( \frac{10^5}{\hat{\beta}_{\max}} \right)^{\frac{1}{2}} \left( \frac{a_{\text{RH}}/a_{\max}}{10^2} \right)^{\frac{3}{2}}, \end{aligned} \quad (10)$$

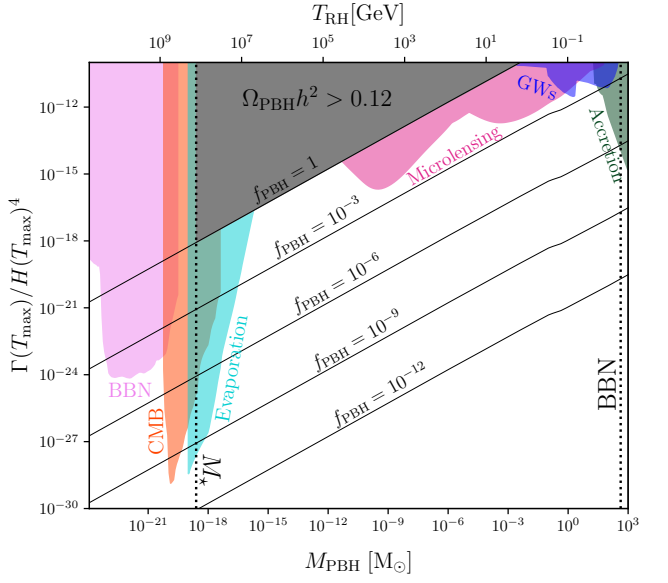


FIG. 3. Fraction of the dark matter relic density that is composed of PBHs, as a function of the PBH mass or equivalently the reheating temperature, using the benchmark values  $\alpha = 0.1$ ,  $a_{\text{RH}}/a_{\max} = 10^2$  and  $\hat{\beta}_{\max} = 10^5$ . Shaded areas correspond to regions of the parameter space excluded by BBN, CMB anisotropies, cosmic-ray detection, microlensing, gravitational wave detection and accretion (as reported in [3]).

where the observed dark matter relic abundance is taken to be  $\rho_{\text{DM}}/s \simeq 0.4 \text{ eV}$  [100].

In Fig. 3, we depict  $\Gamma(T_{\max})/H_{\max}^4$  required to give a sizable  $f_{\text{PBH}}$  for different  $M_{\text{PBH}}$  (or  $T_{\text{RH}}$ ) for  $\alpha = 0.1$ ,  $a_{\text{RH}}/a_{\max} = 10^2$  and  $\hat{\beta}_{\max} = 10^5$ , taking  $g_*(T)$  to be the Standard Model value [101]. We also show relevant constraints coming from the null observation of PBH evaporation signal (cyan), lensing by PBHs (purple), gravitational waves (blue), and accretion (green), taken from Ref. [3]. The dotted line on the right edge represents the lower bound of  $T_{\text{RH}} \gtrsim 5 \text{ MeV}$  (and thus an upper bound of  $M_{\text{PBH}}$ ) coming from the big bang nucleosynthesis [102–107] while the one on the left edge depicts the critical PBH mass  $M_{\star} \simeq 5 \times 10^{14}$  gram below which PBHs evaporate completely before the present [108, 109]. For masses smaller than  $M_{\star}$ , we also indicate constraints from BBN (pink) and CMB anisotropies (orange) on evaporating PBHs [3]. As one can see from this figure, a broad range of values for  $\Gamma(T_{\max})/H_{\max}^4$  lead to an abundance of PBHs that is of phenomenological interest, including PBHs that could constitute the whole dark matter of our Universe.

**Summary and Discussion**—In this *Letter*, we have proposed a new PBH formation mechanism in aborted phase transition during reheating. A symmetry-restoring bubble is nucleated and expands during  $T > T_c$ , and it shrinks back as the temperature drops below  $T_c$ . This generates a macroscopic size of over-density perturbation with a spherical symmetry, which eventually collapses

into a PBH via the post-collapse accretion mechanism during matter domination. The mass of PBHs formed in this process grows quickly by absorbing the surrounding matter, and its final mass is determined by  $T_{\text{RH}}$  as given in Eq. (3). We estimate the PBH abundance (10) in terms of the bubble nucleation rate around  $T_{\text{max}}$  parametrized by the effective rapidity parameter  $\hat{\beta}_{\text{max}}$  at  $T_{\text{max}}$ , and show that it can be sizable in the aspect of phenomenology.

Our findings rely on the post-collapse accretion mechanism [82–84], in which a small overdensity accretes the matter present in the Hubble patch during a matter-dominated era, leading to the formation of a black hole. However, the formation of the black hole and its mass growth may be partially impeded by the velocity dispersion that can be either from the inhomogeneity of the surrounding matter or the non-sphericity of the initial density fluctuation as discussed in Refs. [83, 84, 88, 91]. In our case, the spherical symmetry is guaranteed because the bubble nucleation rate is maximized at an  $O(3)$

symmetric profile along the transition surface in the field configuration space (see, e.g. Ref. [99] and references therein). We expect that even if small non-sphericities exist during nucleation, they get smoothed out due to the interaction of the bubble with the background quasi-homogeneous plasma during its expansion and contraction dynamics. It is also conceivable that a velocity dispersion of matter (the reheaton in our case) may arise from the small inhomogeneities generated during inflation. We leave a detailed investigation of all these effects for future work.

## ACKNOWLEDGMENTS

We thank Shao-Jiang Wang for the helpful discussions. The work of WYA was supported by EPSRC [Grant No. EP/V002821/1]. The work of LH is supported by the STFC (grant No. ST/X000753/1). The work of THJ was supported by IBS under the project code, IBS-R018-D1.

---

[1] A. Escrivà, F. Kuhnel, and Y. Tada, (2022), 10.1016/B978-0-32-395636-9.00012-8, arXiv:2211.05767 [astro-ph.CO].

[2] B. Carr, K. Kohri, Y. Sendouda, and J. Yokoyama, *Rept. Prog. Phys.* **84**, 116902 (2021), arXiv:2002.12778 [astro-ph.CO].

[3] J. Auffinger, *Prog. Part. Nucl. Phys.* **131**, 104040 (2023), arXiv:2206.02672 [astro-ph.CO].

[4] G. F. Chapline, *Nature* **253**, 251 (1975).

[5] P. Ivanov, P. Naselsky, and I. Novikov, *Phys. Rev. D* **50**, 7173 (1994).

[6] B. Carr, F. Kuhnel, and M. Sandstad, *Phys. Rev. D* **94**, 083504 (2016), arXiv:1607.06077 [astro-ph.CO].

[7] T. X. Tran, S. R. Geller, B. V. Lehmann, and D. I. Kaiser, (2023), arXiv:2312.17217 [astro-ph.CO].

[8] A. Loeb, *Res. Notes AAS* **8**, 211 (2024), arXiv:2408.10799 [hep-ph].

[9] B. Carr, S. Clesse, J. García-Bellido, and F. Kühnel, *Phys. Dark Univ.* **31**, 100755 (2021), arXiv:1906.08217 [astro-ph.CO].

[10] B. P. Abbott *et al.* (LIGO Scientific, Virgo), *Phys. Rev. X* **6**, 041015 (2016), [Erratum: *Phys. Rev. X* 8, 039903 (2018)], arXiv:1606.04856 [gr-qc].

[11] R. Abbott *et al.* (KAGRA, VIRGO, LIGO Scientific), *Phys. Rev. X* **13**, 041039 (2023), arXiv:2111.03606 [gr-qc].

[12] S. Bird, I. Cholis, J. B. Muñoz, Y. Ali-Haimoud, M. Kamionkowski, E. D. Kovetz, A. Raccanelli, and A. G. Riess, *Phys. Rev. Lett.* **116**, 201301 (2016), arXiv:1603.00464 [astro-ph.CO].

[13] A. A. Starobinsky, *JETP Lett.* **55**, 489 (1992).

[14] P. Ivanov, *Phys. Rev. D* **57**, 7145 (1998), arXiv:astro-ph/9708224.

[15] J. García-Bellido and E. Ruiz Morales, *Phys. Dark Univ.* **18**, 47 (2017), arXiv:1702.03901 [astro-ph.CO].

[16] J. M. Ezquiaga, J. García-Bellido, and E. Ruiz Morales, *Phys. Lett. B* **776**, 345 (2018), arXiv:1705.04861 [astro-ph.CO].

[17] H. Motohashi and W. Hu, *Phys. Rev. D* **96**, 063503 (2017), arXiv:1706.06784 [astro-ph.CO].

[18] G. Ballesteros and M. Taoso, *Phys. Rev. D* **97**, 023501 (2018), arXiv:1709.05565 [hep-ph].

[19] M. Cicoli, V. A. Diaz, and F. G. Pedro, *JCAP* **06**, 034 (2018), arXiv:1803.02837 [hep-th].

[20] C. T. Byrnes, P. S. Cole, and S. P. Patil, *JCAP* **06**, 028 (2019), arXiv:1811.11158 [astro-ph.CO].

[21] D. Y. Cheong, S. M. Lee, and S. C. Park, *JCAP* **01**, 032 (2021), arXiv:1912.12032 [hep-ph].

[22] G. Ballesteros, J. Rey, M. Taoso, and A. Urbano, *JCAP* **07**, 025 (2020), arXiv:2001.08220 [astro-ph.CO].

[23] J. Yokoyama, *Phys. Rev. D* **58**, 083510 (1998), arXiv:astro-ph/9802357.

[24] V. Briaud and V. Vennin, *JCAP* **06**, 029 (2023), arXiv:2301.09336 [astro-ph.CO].

[25] L. Heurtier, A. Moursy, and L. Wacquez, *JCAP* **03**, 020 (2023), arXiv:2207.11502 [hep-th].

[26] S. S. Mishra and V. Sahni, *JCAP* **04**, 007 (2020), arXiv:1911.00057 [gr-qc].

[27] J. García-Bellido, A. D. Linde, and D. Wands, *Phys. Rev. D* **54**, 6040 (1996), arXiv:astro-ph/9605094.

[28] M. Kawasaki, N. Sugiyama, and T. Yanagida, *Phys. Rev. D* **57**, 6050 (1998), arXiv:hep-ph/9710259.

[29] M. Kawasaki and T. Yanagida, *Phys. Rev. D* **59**, 043512 (1999), arXiv:hep-ph/9807544.

[30] M. Kawasaki, T. Takayama, M. Yamaguchi, and J. Yokoyama, *Phys. Rev. D* **74**, 043525 (2006), arXiv:hep-ph/0605271.

[31] T. Kawaguchi, M. Kawasaki, T. Takayama, M. Yamaguchi, and J. Yokoyama, *Mon. Not. Roy. Astron. Soc.* **388**, 1426 (2008), arXiv:0711.3886 [astro-ph].

[32] P. H. Frampton, M. Kawasaki, F. Takahashi, and T. T. Yanagida, *JCAP* **04**, 023 (2010), arXiv:1001.2308 [hep-ph].

[33] M. Kawasaki, A. Kusenko, and T. T. Yanagida, *Phys.*

Lett. B **711**, 1 (2012), arXiv:1202.3848 [astro-ph.CO].

[34] S. Clesse and J. Garcia-Bellido, Phys. Rev. D **92**, 023524 (2015), arXiv:1501.07565 [astro-ph.CO].

[35] M. Kawasaki, A. Kusenko, Y. Tada, and T. T. Yanagida, Phys. Rev. D **94**, 083523 (2016), arXiv:1606.07631 [astro-ph.CO].

[36] K. Inomata, M. Kawasaki, K. Mukaida, Y. Tada, and T. T. Yanagida, Phys. Rev. D **95**, 123510 (2017), arXiv:1611.06130 [astro-ph.CO].

[37] K. Inomata, M. Kawasaki, K. Mukaida, Y. Tada, and T. T. Yanagida, Phys. Rev. D **96**, 043504 (2017), arXiv:1701.02544 [astro-ph.CO].

[38] Y. Tada and S. Yokoyama, Phys. Rev. D **100**, 023537 (2019), arXiv:1904.10298 [astro-ph.CO].

[39] G. Ballesteros, J. Beltran Jimenez, and M. Pieroni, JCAP **06**, 016 (2019), arXiv:1811.03065 [astro-ph.CO].

[40] G. Ballesteros, S. Céspedes, and L. Santoni, JHEP **01**, 074 (2022), arXiv:2109.00567 [hep-th].

[41] G. A. Palma, S. Sypsas, and C. Zenteno, Phys. Rev. Lett. **125**, 121301 (2020), arXiv:2004.06106 [astro-ph.CO].

[42] J. Fumagalli, S. Renaux-Petel, J. W. Ronayne, and L. T. Witkowski, Phys. Lett. B **841**, 137921 (2023), arXiv:2004.08369 [hep-th].

[43] J. Yokoyama, Astron. Astrophys. **318**, 673 (1997), arXiv:astro-ph/9509027.

[44] M. Kawasaki, N. Kitajima, and T. T. Yanagida, Phys. Rev. D **87**, 063519 (2013), arXiv:1207.2550 [hep-ph].

[45] K. Kohri, C.-M. Lin, and T. Matsuda, Phys. Rev. D **87**, 103527 (2013), arXiv:1211.2371 [hep-ph].

[46] S. Pi and M. Sasaki, Phys. Rev. D **108**, L101301 (2023), arXiv:2112.12680 [astro-ph.CO].

[47] A. Linde, S. Mooij, and E. Pajer, Phys. Rev. D **87**, 103506 (2013), arXiv:1212.1693 [hep-th].

[48] Y.-F. Cai, X. Tong, D.-G. Wang, and S.-F. Yan, Phys. Rev. Lett. **121**, 081306 (2018), arXiv:1805.03639 [astro-ph.CO].

[49] R.-G. Cai, Z.-K. Guo, J. Liu, L. Liu, and X.-Y. Yang, JCAP **06**, 013 (2020), arXiv:1912.10437 [astro-ph.CO].

[50] A. M. Green and K. A. Malik, Phys. Rev. D **64**, 021301 (2001), arXiv:hep-ph/0008113.

[51] B. A. Bassett and S. Tsujikawa, Phys. Rev. D **63**, 123503 (2001), arXiv:hep-ph/0008328.

[52] J. Martin, T. Papanikolaou, and V. Vennin, JCAP **01**, 024 (2020), arXiv:1907.04236 [astro-ph.CO].

[53] J. Martin, T. Papanikolaou, L. Pinol, and V. Vennin, JCAP **05**, 003 (2020), arXiv:2002.01820 [astro-ph.CO].

[54] G. Ballesteros, J. Iguaz Juan, P. D. Serpico, and M. Taoso, (2024), arXiv:2406.09122 [astro-ph.CO].

[55] H. Kodama, M. Sasaki, and K. Sato, Prog. Theor. Phys. **68**, 1979 (1982).

[56] S. W. Hawking, I. G. Moss, and J. M. Stewart, Phys. Rev. D **26**, 2681 (1982).

[57] J. Garriga, A. Vilenkin, and J. Zhang, JCAP **02**, 064 (2016), arXiv:1512.01819 [hep-th].

[58] J. Liu, L. Bian, R.-G. Cai, Z.-K. Guo, and S.-J. Wang, Phys. Rev. D **105**, L021303 (2022), arXiv:2106.05637 [astro-ph.CO].

[59] C. Gross, G. Landini, A. Strumia, and D. Teresi, JHEP **09**, 033 (2021), arXiv:2105.02840 [hep-ph].

[60] M. J. Baker, M. Breitbach, J. Kopp, and L. Mittnacht, (2021), arXiv:2105.07481 [astro-ph.CO].

[61] K. Kawana and K.-P. Xie, Phys. Lett. B **824**, 136791 (2022), arXiv:2106.00111 [astro-ph.CO].

[62] T. H. Jung and T. Okui, (2021), arXiv:2110.04271 [hep-ph].

[63] H. Deng and A. Vilenkin, JCAP **12**, 044 (2017), arXiv:1710.02865 [gr-qc].

[64] K. Hashino, S. Kanemura, and T. Takahashi, Phys. Lett. B **833**, 137261 (2022), arXiv:2111.13099 [hep-ph].

[65] M. J. Baker, M. Breitbach, J. Kopp, and L. Mittnacht, (2021), arXiv:2110.00005 [astro-ph.CO].

[66] P. Huang and K.-P. Xie, Phys. Rev. D **105**, 115033 (2022), arXiv:2201.07243 [hep-ph].

[67] S. He, L. Li, Z. Li, and S.-J. Wang, Sci. China Phys. Mech. Astron. **67**, 240411 (2024), arXiv:2210.14094 [hep-ph].

[68] K. Kawana, T. Kim, and P. Lu, Phys. Rev. D **108**, 103531 (2023), arXiv:2212.14037 [astro-ph.CO].

[69] M. Lewicki, P. Toczek, and V. Vaskonen, JHEP **09**, 092 (2023), arXiv:2305.04924 [astro-ph.CO].

[70] Y. Gouttenoire and T. Volansky, Phys. Rev. D **110**, 043514 (2024), arXiv:2305.04942 [hep-ph].

[71] I. Baldes and M. O. Olea-Romacho, JHEP **01**, 133 (2024), arXiv:2307.11639 [hep-ph].

[72] Y. Gouttenoire, Phys. Lett. B **855**, 138800 (2024), arXiv:2311.13640 [hep-ph].

[73] M. Lewicki, P. Toczek, and V. Vaskonen, (2024), arXiv:2402.04158 [astro-ph.CO].

[74] M. M. Flores, A. Kusenko, and M. Sasaki, Phys. Rev. D **110**, 015005 (2024), arXiv:2402.13341 [hep-ph].

[75] S. Kanemura, M. Tanaka, and K.-P. Xie, JHEP **06**, 036 (2024), arXiv:2404.00646 [hep-ph].

[76] R.-G. Cai, Y.-S. Hao, and S.-J. Wang, (2024), arXiv:2404.06506 [astro-ph.CO].

[77] D. Gonçalves, A. Kaladharan, and Y. Wu, (2024), arXiv:2406.07622 [hep-ph].

[78] M. A. Buen-Abad, J. H. Chang, and A. Hook, Phys. Rev. D **108**, 036006 (2023), arXiv:2305.09712 [hep-ph].

[79] A. Azatov, G. Barni, and R. Petrossian-Byrne, (2024), arXiv:2405.19447 [hep-ph].

[80] G. Barni, S. Blasi, and M. Vanvlasselaer, (2024), arXiv:2406.01596 [hep-ph].

[81] D. J. H. Chung, E. W. Kolb, and A. Riotto, Phys. Rev. D **60**, 063504 (1999), arXiv:hep-ph/9809453.

[82] E. de Jong, J. C. Aurrekoetxea, and E. A. Lim, JCAP **03**, 029 (2022), arXiv:2109.04896 [astro-ph.CO].

[83] V. De Luca, G. Franciolini, A. Kehagias, P. Pani, and A. Riotto, Phys. Lett. B **832**, 137265 (2022), arXiv:2112.02534 [astro-ph.CO].

[84] E. de Jong, J. C. Aurrekoetxea, E. A. Lim, and T. França, JCAP **10**, 067 (2023), arXiv:2306.11810 [astro-ph.CO].

[85] M. Y. Khlopov and A. G. Polnarev, Phys. Lett. B **97**, 383 (1980).

[86] M. Y. Khlopov, B. A. Malomed, I. B. Zeldovich, and Y. B. Zeldovich, Mon. Not. Roy. Astron. Soc. **215**, 575 (1985).

[87] T. Harada, C.-M. Yoo, and K. Kohri, Phys. Rev. D **88**, 084051 (2013), [Erratum: Phys. Rev. D **89**, 029903 (2014)], arXiv:1309.4201 [astro-ph.CO].

[88] T. Harada, C.-M. Yoo, K. Kohri, K.-i. Nakao, and S. Jhingan, Astrophys. J. **833**, 61 (2016), arXiv:1609.01588 [astro-ph.CO].

[89] T. Harada, C.-M. Yoo, K. Kohri, and K.-i. Nakao, Phys. Rev. D **96**, 083517 (2017), [Erratum: Phys. Rev. D **99**, 069904 (2019)], arXiv:1707.03595 [gr-qc].

[90] T. Kokubu, K. Kyutoku, K. Kohri, and T. Harada,

Phys. Rev. D **98**, 123024 (2018), arXiv:1810.03490 [astro-ph.CO].

[91] T. Harada, K. Kohri, M. Sasaki, T. Terada, and C.-M. Yoo, JCAP **02**, 038 (2023), arXiv:2211.13950 [astro-ph.CO].

[92] J. C. Hidalgo, J. De Santiago, G. German, N. Barbosa-Cendejas, and W. Ruiz-Luna, Phys. Rev. D **96**, 063504 (2017), arXiv:1705.02308 [astro-ph.CO].

[93] B. Carr, T. Tenkanen, and V. Vaskonen, Phys. Rev. D **96**, 063507 (2017), arXiv:1706.03746 [astro-ph.CO].

[94] B. Carr, K. Dimopoulos, C. Owen, and T. Tenkanen, Phys. Rev. D **97**, 123535 (2018), arXiv:1804.08639 [astro-ph.CO].

[95] R. Allahverdi *et al.*, (2020), 10.21105/astro.2006.16182, arXiv:2006.16182 [astro-ph.CO].

[96] K. Carrion, J. C. Hidalgo, A. Montiel, and L. E. Padilla, JCAP **07**, 001 (2021), arXiv:2101.02156 [astro-ph.CO].

[97] A. D. Linde, Phys. Lett. B **100**, 37 (1981).

[98] A. D. Linde, Nucl. Phys. B **216**, 421 (1983), [Erratum: Nucl.Phys.B 223, 544 (1983)].

[99] O. Gould and J. Hirvonen, Phys. Rev. D **104**, 096015 (2021), arXiv:2108.04377 [hep-ph].

[100] N. Aghanim *et al.* (Planck), Astron. Astrophys. **641**, A6 (2020), [Erratum: Astron.Astrophys. 652, C4 (2021)], arXiv:1807.06209 [astro-ph.CO].

[101] K. Saikawa and S. Shirai, JCAP **05**, 035 (2018), arXiv:1803.01038 [hep-ph].

[102] M. Kawasaki, K. Kohri, and N. Sugiyama, Phys. Rev. Lett. **82**, 4168 (1999), arXiv:astro-ph/9811437.

[103] M. Kawasaki, K. Kohri, and N. Sugiyama, Phys. Rev. D **62**, 023506 (2000), arXiv:astro-ph/0002127.

[104] S. Hannestad, Phys. Rev. D **70**, 043506 (2004), arXiv:astro-ph/0403291.

[105] K. Ichikawa, M. Kawasaki, and F. Takahashi, Phys. Rev. D **72**, 043522 (2005), arXiv:astro-ph/0505395.

[106] P. F. de Salas, M. Lattanzi, G. Mangano, G. Miele, S. Pastor, and O. Pisanti, Phys. Rev. D **92**, 123534 (2015), arXiv:1511.00672 [astro-ph.CO].

[107] T. Hasegawa, N. Hiroshima, K. Kohri, R. S. L. Hansen, T. Tram, and S. Hannestad, JCAP **12**, 012 (2019), arXiv:1908.10189 [hep-ph].

[108] B. J. Carr, K. Kohri, Y. Sendouda, and J. Yokoyama, Phys. Rev. D **81**, 104019 (2010), arXiv:0912.5297 [astro-ph.CO].

[109] B. J. Carr, K. Kohri, Y. Sendouda, and J. Yokoyama, Phys. Rev. D **94**, 044029 (2016), arXiv:1604.05349 [astro-ph.CO].

[110] S. R. Coleman and E. J. Weinberg, Phys. Rev. D **7**, 1888 (1973).

[111] C. L. Wainwright, Comput. Phys. Commun. **183**, 2006 (2012), arXiv:1109.4189 [hep-ph].

[112] B.-H. Liu, L. D. McLerran, and N. Turok, Phys. Rev. D **46**, 2668 (1992).

[113] G. D. Moore and T. Prokopec, Phys. Rev. Lett. **75**, 777 (1995), arXiv:hep-ph/9503296.

[114] G. D. Moore and T. Prokopec, Phys. Rev. D **52**, 7182 (1995), arXiv:hep-ph/9506475.

[115] T. Konstandin, G. Nardini, and I. Rues, JCAP **09**, 028 (2014), arXiv:1407.3132 [hep-ph].

[116] W.-Y. Ai, B. Garbrecht, and C. Tamarit, JCAP **03**, 015 (2022), arXiv:2109.13710 [hep-ph].

[117] D. Bodeker and G. D. Moore, JCAP **05**, 009 (2009), arXiv:0903.4099 [hep-ph].

[118] W.-Y. Ai, X. Nagels, and M. Vanvlasselaer, JCAP **03**, 037 (2024), arXiv:2401.05911 [hep-ph].

[119] D. Bodeker and G. D. Moore, JCAP **05**, 025 (2017), arXiv:1703.08215 [hep-ph].

[120] S. Höche, J. Kozaczuk, A. J. Long, J. Turner, and Y. Wang, JCAP **03**, 009 (2021), arXiv:2007.10343 [hep-ph].

[121] A. Azatov and M. Vanvlasselaer, JCAP **01**, 058 (2021), arXiv:2010.02590 [hep-ph].

[122] Y. Gouttenoire, R. Jinno, and F. Sala, JHEP **05**, 004 (2022), arXiv:2112.07686 [hep-ph].

[123] W.-Y. Ai, JCAP **10**, 052 (2023), arXiv:2308.10679 [hep-ph].

[124] A. Azatov, G. Barni, R. Petrossian-Byrne, and M. Vanvlasselaer, JHEP **05**, 294 (2024), arXiv:2310.06972 [hep-ph].

[125] A. J. Long and J. Turner, (2024), arXiv:2407.18196 [hep-ph].

[126] J. M. Cline, A. Friedlander, D.-M. He, K. Kainulainen, B. Laurent, and D. Tucker-Smith, Phys. Rev. D **103**, 123529 (2021), arXiv:2102.12490 [hep-ph].

[127] B. Laurent and J. M. Cline, Phys. Rev. D **106**, 023501 (2022), arXiv:2204.13120 [hep-ph].

[128] W.-Y. Ai, B. Laurent, and J. van de Vis, JCAP **07**, 002 (2023), arXiv:2303.10171 [astro-ph.CO].

## Supplemental Material

### S1. AN EXAMPLE MODEL TO EVALUATE THE PHASE TRANSITION RAPIDITY PARAMETER

In this section, we consider a benchmark model and obtain  $\hat{\beta}_{\max}$ . The model we consider is a simple Abelian Higgs model where a complex scalar field  $\Phi$  is charged under a  $U(1)$  gauge interaction with a charge unity. We further assume that the theory is classically scale invariant, so the tree-level potential is given by

$$V(\Phi) = \lambda|\Phi|^4, \quad (\text{S1})$$

where  $\lambda$  is the self-quartic coupling. The spontaneous symmetry breaking is radiatively generated as originally shown in Ref. [110].

To include the loop effects conveniently, we take the RG scale  $\mu = \mu_*$  which is defined by  $\lambda(\mu_*) = 0$ . The existence of such  $\mu_*$  is guaranteed by the positive beta function of  $\lambda$  coming from the gauge boson loop. Denoting  $\phi$  for the radial degree of  $\Phi$ , the one-loop effective potential can be written as

$$V(\phi) = \frac{\delta\lambda}{4}\phi^4 + \frac{1}{4}\beta_\lambda\phi^4 \log \frac{\phi}{\mu_*}, \quad (\text{S2})$$

where  $\delta\lambda = \frac{3g^4}{16\pi^2}(\log g^2 - 5/6)$  and  $\beta_\lambda = 6g^4/16\pi^2$  with  $g$  being the gauge coupling. This potential is minimized at  $v_\phi = e^{1/6}\mu_*/g$  and the potential energy difference is given by  $\Delta V_0 = \frac{3e^{2/3}}{128\pi^2}\mu_*^4$ .

We include the thermal correction coming from the gauge boson loop,

$$\Delta V_{T \neq 0} = \frac{3T^4}{2\pi^2} J_B(m_V^2/T^2), \quad (\text{S3})$$

with the field-dependent gauge boson mass  $m_V = g\phi$  and the  $J_B$  function given by

$$J_B(y^2) = \int_0^\infty dx x^2 \log \left[ 1 - e^{-\sqrt{x^2+y^2}} \right]. \quad (\text{S4})$$

Note that the scalar-loop contribution vanishes due to our choice of RG scale,  $\lambda(\mu_*) = 0$ .

In this specific setup, we find two important model properties. First,  $T_c$  is independent of the size of gauge coupling  $g$  since the zero-temperature potential energy difference is given by  $\Delta V_0 = \frac{3e^{2/3}}{128\pi^2}\mu_*^4$  independently of  $g$ . Second, the binodal temperature  $T_1$  (where the potential barrier disappears) is also  $g$ -independent. This is because the effective field range of the thermal correction  $\phi_{\text{eff},T}$  has the same coupling dependence with  $v_\phi \sim \mu_*/g$ ;  $\phi_{\text{eff},T}$  can be estimated by  $m_V(\phi_{\text{eff},T}) \sim T$ , so  $\phi_{\text{eff},T} \sim T/g$ . We numerically find that  $T_c \simeq 0.37\mu_*$  and  $T_1 \simeq 0.44\mu_*$ . For our PBH formation scenario,  $T_{\max}$  must be between  $T_1$  and  $T_c$ , which is not impossible although it requires tuning (note that there are already multiple coincidences of time scales in the standard cosmology).

These properties can be changed by including additional fields. For instance, if we include a Dirac fermion  $\psi$  that couples to  $\phi$  via a Yukawa interaction,  $T_c$  decreases while  $T_1$  does not change much. This can increase the ratio of  $T_1$  and  $T_c$ , reducing the required level of tuning  $T_{\max}$ .

For a temperature between  $T_c$  and  $T_1$ , we obtain the bounce action by using the CosmoTransitions [111]. The result of  $S_3/T$  is given in the left panel of Fig. S4. Then, we obtain the rapidity parameter as shown in the right panel of Fig. S4, which shows that  $10^4 \lesssim \hat{\beta}_{\max} \lesssim 10^6$ .

### S2. DYNAMICS OF A SYMMETRY-RESTORING BUBBLE

In this section, we show that the bubble wall typically reaches a terminal velocity, i.e., has a non-runaway behavior, in both the expansion and contraction stages. Bubble wall dynamics is a highly complicated subject, requiring one to solve the Boltzmann equations for the particle distribution functions (which are integro-differential equations), the background scalar equation of motion, and the fluid equations for the hydrodynamics [112–116]. To determine whether or not a bubble wall runs away, i.e. accelerates all the way until colliding with another bubble, friction in the  $\gamma_w \rightarrow \infty$  limit is usually compared to the vacuum energy difference [117] (although this may not always be valid [118]). Below, we also do a similar analysis, using the simple Bödeker-Moore criterion [117].

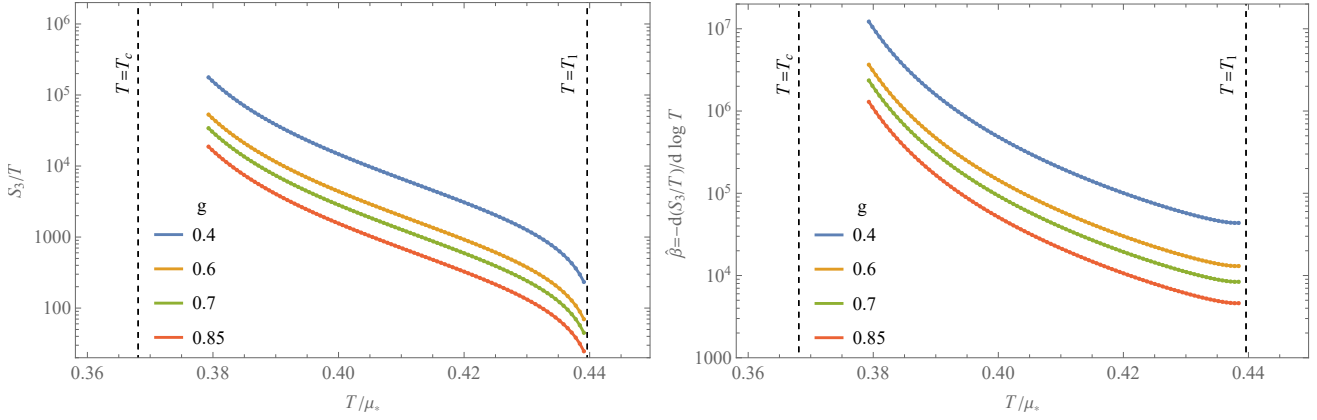


FIG. S4. Our numerical result of  $S_3/T$  and  $\hat{\beta} = -d(S_3/T)/d \ln T$  for the Abelian Higgs model.

### A. Bubble expansion ( $T > T_c$ )

Let us first consider bubble expansion. Note that, for  $T > T_c$ , the vacuum energy inside the bubble is greater than outside, i.e.  $\Delta V_0 < 0$ , so the vacuum energy always gives a negative pressure that tries to contract the bubble. On the other hand, the thermal pressure difference  $\Delta V_{T \neq 0}$  is positive, and this is the driving force of the bubble expansion. When a bubble is formed at  $T > T_c$ , the bubble wall gets accelerated since the net pressure is positive (by the definition of  $T_c$ ). When the bubble wall velocity is nonzero, the thermal driving force is reduced. This can be seen from the fact that, in the example of 1-to-1 transmission processes, the momentum transfer in the wall-rest frame decreases as the fluid velocity increases;  $\Delta p_z = \sqrt{p_z^2 + \Delta m^2} - p_z \sim \Delta m^2/2p_z$  where  $z$  is the direction of the bubble wall propagation,  $p_z$  is the momentum of a particle coming toward the bubble wall from outside, and  $\Delta m^2 > 0$  is the mass-squared difference. Therefore, as velocity increases, the thermal driving force decreases until it reaches the equilibrium with the vacuum energy pressure.

As pointed out in Ref. [80], the thermal driving force has a nonzero asymptotic value in  $v_w \rightarrow \infty$  limit, which we also call Bödeker-Moore thermal force

$$\mathcal{P}_{\text{BM}} = \sum_i C_i g_i c_i \frac{\Delta m_i^2 T^2}{24}, \quad (\text{S5})$$

where  $c_i = 1(1/2)$  for bosons (fermions). Here  $g_i$  is the number of internal degrees of freedom of species  $i$  that couple with the scalar  $\phi$ , and  $\Delta m_i^2$  is the difference of the squared-mass in broken and symmetric phases.  $C_i$  is approximately given by

$$\frac{C_i T^2}{24} \approx \begin{cases} \frac{T^2}{24} & \text{if } m_i^{\text{out}} \ll T, \\ \frac{1}{2m_i^{\text{out}}} \left( \frac{m_i^{\text{out}} T}{2\pi} \right)^{3/2} e^{-m_i^{\text{out}}/T} & \text{if } m_i^{\text{out}} \gg T, \end{cases} \quad (\text{S6})$$

with  $m_i^{\text{out}}$  being the mass outside of the wall, i.e. in the broken phase.

If  $m_i^{\text{out}}$  are larger than the temperature, which is the case for our model considered in the last section,  $\mathcal{P}_{\text{BM}}$  would be suppressed because the number density of those heavy particles is Boltzmann-suppressed. This means that the asymptotic value of the driving force is small, ensuring the existence of equilibrium with  $\Delta V_0$  at some velocity.

We note that  $\mathcal{P}_{\text{BM}}$  is the force caused only by the  $1 \rightarrow 1$  processes. There can be additional forces caused by particle-production processes [119–125], i.e., when a particle splits into two or more particles when it transits across the wall. These next-to-leading-order forces may behave as true friction as in a cooling phase transition [79]. We also note that hydrodynamic effects can induce a barrier of the frictional pressure at the Jouguet velocity [118, 126–128]. All these factors would just make our conclusion more solid.

### B. Bubble contraction ( $T < T_c$ )

For  $T < T_c$ , the dynamics of the bubble wall can be understood in the usual way although our bubble is still symmetry-restoring and contracts. Actually, the contraction process under consideration can be likened to the contraction of a *false-vacuum* bubble (sometimes referred to as a *false-vacuum island*) in a cooling and symmetry-breaking

FOPT. During contraction, the vacuum energy difference accelerates the bubble wall velocity while the thermal effect acts as friction. In this case, when the wall velocity increases, the friction increases and has an asymptotic value of  $\mathcal{P}_{\text{BM}}$  [117]. Thus, if  $|\Delta V_0| < \mathcal{P}_{\text{BM}}$ , there exists a terminal velocity where the friction and  $\Delta V_0$  make an equilibrium.

Before proceeding, note that the temperature range in our process is all around  $T_c$ . As shown in the previous section,  $T_{\text{max}}/T_c < T_1/T_c$  cannot be large in the model-building aspect, and therefore, the temperature when the bubble shrinks and disappears, which we denote  $T_{\text{zero}}$ , should be also close to  $T_c$ .

Now let us again consider the large- $\gamma_w$  limit. In bubble contraction, the driving force is

$$\mathcal{P}_{\text{driving}} = |\Delta V_0|, \quad (\text{S7})$$

while the Bodeker-Moore thermal force is [117]

$$\mathcal{P}_{\text{friction}} = \mathcal{P}_{\text{BM}} = \sum_i g_i c_i \frac{\Delta m^2 T^2}{24} \sim g_{\star, \phi} \frac{\Delta m^2 T^2}{24}, \quad (\text{S8})$$

is a true friction where  $g_{\star, \phi}$  is the effective degrees of freedom that couple to  $\phi$ .

On the other hand, we have the relation of  $\Delta V_0 \simeq g_{\star, \phi} \frac{\pi^2}{90} T_c^4$  which is smaller than  $\mathcal{P}_{\text{BM}}$  for  $\Delta m^2 > T^2$ . Therefore, we conclude that the bubble wall still does not run away even without taking into account friction from 1-to-2 or 1-to-many processes and hydrodynamic obstruction [118].